

# Localization and Superconductivity in Doped Semiconductors

Youichi YANASE\* and Naoyuki Yorozu

*Department of Physics, University of Tokyo, Tokyo 113-0033, Japan*

(Received 14. Oct. 2008)

Motivated by the discovery of superconductivity in boron-doped (B-doped) diamond, we investigate the localization and superconductivity in heavily doped semiconductors. The competition between Anderson localization and  $s$ -wave superconductivity is investigated from the microscopic point of view. The effect of microscopic inhomogeneity and the thermal fluctuation in superconductivity are taken into account using the self-consistent 1-loop-order theory with respect to superconducting fluctuation. The crossover from superconductivity in the host band to that in the impurity band is described on the basis of the disordered three-dimensional attractive Hubbard model for binary alloys. We show that superconductor-insulator transition (SIT) accompanies the crossover. We point out an enhancement of Cooper pairing in the crossover regime. Further localization of the electron wave function gives rise to incoherent Cooper pairs and the pseudogap above  $T_c$ . A global phase diagram is drawn for host band superconductivity, impurity band superconductivity, Anderson localization, Fermi liquid state, and pseudogap state. A theoretical interpretation is proposed for superconductivity in the doped diamond, SiC, and Si.

**KEYWORDS:** Anderson localization; superconductor-insulator-transition; localized Cooper pairs; heavily doped semiconductors

## 1. Introduction

Superconductivity in the vicinity of quantum phase transitions has attracted much interest. Superconductivity in high- $T_c$  cuprates,<sup>1</sup> organic superconductors,<sup>2</sup> and heavy fermions<sup>3</sup> occurs in proximity to various quantum critical points, which has been a central issue in the condensed matter physics. Another classical issue is the SIT, which arises from the competition between Anderson localization<sup>4</sup> and  $s$ -wave superconductivity. Vast theoretical studies have been devoted to the SIT triggered by disorders.<sup>5–16</sup> In this paper, we point out that the recently discovered superconductivity in B-doped diamond<sup>17</sup> and related materials<sup>18–20</sup> provides a new field of superconductivity in the vicinity of Anderson localization.

Diamond is recognized as a precious gem, but becomes a wide-gap semiconductor with light doping with substitutional boron acceptors. Superconductivity has been discovered by Ekimov *et al.* by increasing the concentration of boron acceptors.<sup>17</sup> A transition temperature higher than 10 K has been realized in heavily B-doped diamond.<sup>21,22</sup> It seems to be surprising that such a high transition temperature is induced by low carriers in a three-dimensional system since a small density of states (DOS) near the band edge is harmful for superconductivity. It is highly desired to identify a novel mechanism of the enhancement of superconductivity in B-doped diamond.

Semiconductors have been a central field in experimental studies of Anderson localization.<sup>23</sup> Low carriers in semiconductors are significantly affected by randomness since the electron wave function near the band edge is localized by a weak disorder.<sup>24</sup> The effects of randomness have been actually revealed by experiments on B-doped diamond, which have shown the localization effect,<sup>25</sup> high residual resistivity,<sup>25,26</sup> and absence

of a well-defined Fermi surface.<sup>27</sup> Superconductivity in B-doped diamond is referred as “superconductivity with no Fermi surface”.<sup>28</sup> However, the localization effect has never been investigated in theories of the B-doped diamond.<sup>29–35</sup> The purpose of this study is to investigate the relationship between localization and superconductivity in doped semiconductors.

Two theoretical scenarios have been proposed for superconductivity in B-doped diamond. The first one is based on the impurity band formed by impurity states whose wave functions are localized around boron atoms.<sup>29–31,36</sup> The other is based on the host band of diamond in which the carriers are provided by substitutional boron acceptors.<sup>32–35</sup> The former was proposed by Baskaran<sup>29</sup> immediately after the discovery of superconductivity. The latter has been proposed on the basis of first-principles band calculations.<sup>32–35</sup>

Some experimental studies have been carried out to determine which scenario well describes the electronic structure of B-doped diamond.<sup>25–27,37–39</sup> Although photoemission spectroscopy<sup>25,27</sup> has never observed any indication of the impurity band, the presence of the impurity band has been claimed by optical measurement.<sup>38</sup> We point out here that the two scenarios, namely, superconductivity in the impurity band and that in the host band, are not contradicting concepts, and can be continuously described using a microscopic model. In this study, we examine the crossover from the host band to the impurity band on the basis of the disordered attractive Hubbard model of binary alloys. We show that the crossover is accompanied by the SIT, increases in  $T_c$ , and pseudogap. The crossover in the electric DOS can be described by coherent potential approximation (CPA), which has been applied to the analysis of B-doped diamond.<sup>31</sup> However, the spatial inhomogeneity and fluctuations of superconductivity, which are neglected in the

CPA, play an essential role in superconductivity in the crossover and impurity band regimes.

	C:B	SiC:Al	SiC:B	Si:B
$T_c$ (K)	$> 10$	$\sim 1.5$	$\sim 1.5$	$\sim 0.35$
$H_{c2}$ or $H_c$ (Oe)	$> 10^5$	$\sim 370$	$\sim 115$	?
type	type II	type II	type I	type I

Table I. Superconducting properties of the B-doped diamond, SiC, and Si as well as the Al-doped SiC. The maximum values of  $T_c$ , and  $H_{c2}$  or  $H_c$  are shown. More detailed comparisons have been given in ref. 40.

Boron acceptors also induce superconductivity in Si<sup>18</sup> and SiC.<sup>19</sup> Recently, superconductivity has also been realized in Al-doped SiC.<sup>20</sup> The superconducting properties of these materials are summarized in Table. I. More detailed comparisons between B-doped diamond, SiC and Si have been summarized by Kriener *et al.*<sup>40</sup> The maximum  $T_c$  values are 0.35 K for B-doped Si and 1.5 K for B-doped SiC. A more pronounced difference from B-doped diamond is the magnetic response in the superconducting state. B-doped diamond is a type II superconductor, while the others are type I superconductors. The large Ginzburg-Landau (GL) parameter  $\kappa \sim 18$  of B-doped diamond<sup>26</sup> should be contrasted to the small GL parameter  $\kappa \sim 0.35$  of B-doped SiC.<sup>40</sup> The upper critical field of such diamond is  $10^3$  times higher than the critical field of such SiC. These differences should be related to electronic properties. B-doped diamond is a “bad metal” without any well-defined Fermi surface,<sup>27</sup> while B-doped SiC is a “good metal” with a small residual resistivity.<sup>19,40</sup> We will propose here a theoretical interpretation for the differences between these superconductors.

The paper is organized as follows. The disordered attractive Hubbard model is introduced in §2. The crossover from the impurity band to the host band is demonstrated in §3. We examine the Anderson transition in §4, and the superconductivity is investigated in §5. We discuss B-doped diamond, SiC, and Si in §6. The similarity between the doped semiconductors and the high- $T_c$  cuprates is pointed out in §7. These results are summarized in §8.

## 2. Disordered Attractive Hubbard Model

For a discussion of superconductivity in heavily doped semiconductors, we investigate the disordered attractive Hubbard model in three dimension:

$$H = -t \sum_{\langle i,j \rangle, \sigma} c_{i\sigma}^\dagger c_{j\sigma} + \sum_i (W_i - \mu) n_i + U \sum_i n_{i,\uparrow} n_{i,\downarrow}, \quad (1)$$

where  $n_{i,\sigma}$  is the number of electrons at the site  $i$  with the spin  $\sigma$  and  $n_i = \sum_\sigma n_{i,\sigma}$ . The simple cubic lattice is assumed and the symbol  $\langle i, j \rangle$  denotes the summation over the nearest neighbor sites. We choose the unit of energy as  $t = 1$ .

The disorder is described by the random potential  $W_i$ . We assume a binary alloy in which  $W_i = 0$  at host sites

(carbon sites in B-doped diamond) and  $W_i = U_{\text{imp}}$  at impurity sites (boron sites in B-doped diamond). We denote impurity concentration as  $n_{\text{imp}}$ . The chemical potential  $\mu$  is chosen so that the total electron concentration is  $n = 2 - n_{\text{imp}}$  in accordance with those in B-doped diamond, SiC, and Si. Note that the presence of a B-H complex<sup>41</sup> hardly affects the following results, and therefore  $n_{\text{imp}}$  should be regarded as the concentration of isolated boron atoms. We assume  $n_{\text{imp}} = 0.02$  in §3, §4, and §5.2-5.5, and discuss the doping dependence of superconductivity in §5.6.

It is believed that the electron phonon interaction gives rise to superconductivity in B-doped diamond.<sup>32-35</sup> We take into account the static attractive interaction  $U \leq 0$  to describe the  $s$ -wave pairing interaction for simplicity.

## 3. Crossover from Host Band to Impurity Band

The crossover from the host band to the impurity band is described by varying the impurity potential  $U_{\text{imp}}$  in the model eq. (1). Figure 1 shows the DOS's for various impurity potentials. Here, we assume  $U = 0$  for simplicity.

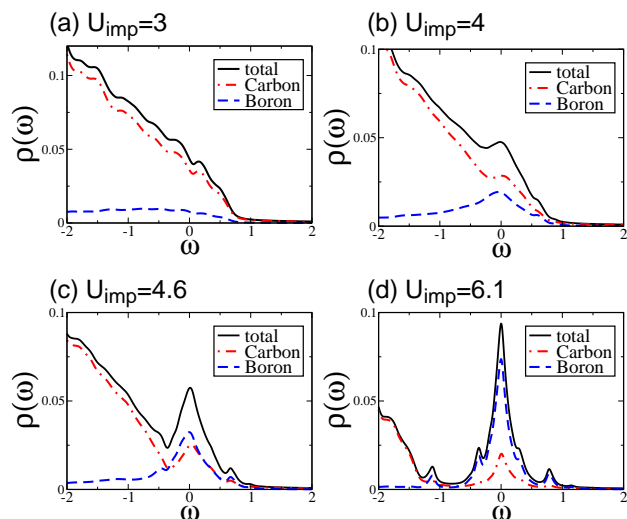


Fig. 1. DOS in the normal state (solid line). We assume  $U_{\text{imp}} = 3, 4, 4.6,$  and  $6.1$  in (a), (b), (c), and (d), respectively. We assume  $n_{\text{imp}} = 0.02$  and  $U = 0$ . The dashed and dash-dotted lines show the partial DOS's in the boron and carbon sites, respectively. The numerical calculation is carried out in  $21^3$  sites. 50 samples are taken for determining the random average.

For a large impurity potential  $U_{\text{imp}} = 6.1$ , the impurity band is clearly separated from the host band, as shown in Fig. 1(d). The holes are nearly half-filled in the impurity band.<sup>31</sup> On the other hand, the impurity band is implanted into the host band for a small impurity potential  $U_{\text{imp}} = 3$ , as shown in Fig. 1(a). Single-particle states around the Fermi level are formed by impurity states in the former, while those are formed by the host band of diamond in the latter. A crossover between the two regimes occurs, and the impurity band merges with the host band at around  $U_{\text{imp}} = 4 \sim 4.6$ , as shown in Figs. 1(b) and 1(c). The acceptor level of the lightly doped boron atoms in diamond has been estimated to be 0.37 eV,<sup>42</sup> which

corresponds to  $U_{\text{imp}} = 4.6$ .<sup>31</sup> Thus, B-doped diamond seems to be near the crossover regime.

#### 4. Anderson Localization

In this section, we investigate Anderson localization in the model eq. (1) to clarify the electronic structure in the normal state, which is a background of superconductivity. We analyze here the inverse participation ratio (IPR) and level statistics for this purpose.

For  $U = 0$ , the Hamiltonian eq. (1) is diagonalized on the basis of the single-particle states. The IPR is defined as

$$\text{IPR} = \langle \langle \sum_{\vec{r}} |\psi_{\alpha}(\vec{r})|^4 \rangle \rangle_{E_F}, \quad (2)$$

where  $\psi_{\alpha}(\vec{r})$  is a single-particle wave function with an energy  $\varepsilon_{\alpha}$ . The bracket  $\langle \rangle_{E_F}$  indicates the average for the states around the Fermi energy,  $|\varepsilon_{\alpha} - \mu| < \varepsilon_c$ . We choose  $\varepsilon_c = 0.2$  so that the cutoff  $\varepsilon_c$  is less than the width of the impurity band. The IPR describes the itinerant or localized character of the single-particle state. The size scaling of the IPR shows  $\text{IPR} \propto N^{-1}$  with  $N$  being the number of sites for the completely extended state, while the IPR is constant for the localized state. We denote here  $N = L^3$  with  $L$  being the linear size of the three-dimensional lattice. The single particle wave function has a fractal dimension  $d^*$  in disordered systems, where  $\text{IPR} \propto N^{-d^*/d}$ . Note that  $d = 3$  in our case. The universal distribution of the fractal dimension  $d^*$  at the mobility edge has been shown.<sup>43</sup> The average is estimated to be  $d^* = 1.3$  for the three-dimensional Anderson transition in the orthogonal universality class.<sup>43</sup>

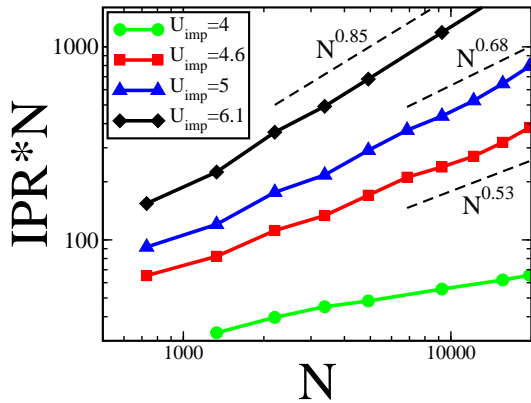


Fig. 2. Size scaling of the IPR for  $U_{\text{imp}} = 4, 4.6, 5$ , and  $6.1$  from the bottom to the top. We assume that  $n_{\text{imp}} = 0.02$  and  $U = 0$ . The power against the size  $N$  is shown as a visual guide. We take into account 220, 150, 100, 70, 50, 40, 30, and 20 samples for  $13^3, 15^3, 17^3, 19^3, 21^3, 23^3, 25^3$ , and  $27^3$  sites, respectively.

Figure 2 shows the scaling plot of the  $\text{IPR} \times N$  for a fixed impurity concentration  $n_{\text{imp}} = 0.02$ . We observe a significant decrease in the fractal dimension  $d^*$  with increasing impurity potential  $U_{\text{imp}}$  through the crossover from the host band to the impurity band. Since the average fractal dimension  $d^* = 1.3$  at the mobility edge leads to the scaling  $\text{IPR} \times N \propto N^{0.57}$ , we find Anderson transition at around  $U_{\text{imp}} = 4.6$ . Thus, the crossover from

the host band to the impurity band is accompanied by Anderson localization. It is reasonable that the single-particle wave function becomes localized with approach to the impurity band regime.

The IPR is also an important index for the superconductivity, because the attractive interaction between the time-reversed states is proportional to the IPR. Since Cooper pairing is determined by this interaction in the localized limit,<sup>11</sup> the data in Fig. 2 implies the enhancement of Cooper pairing with increasing  $U_{\text{imp}}$ . This is qualitatively true, although the parameters assumed here are far from the localized limit. The DOS shown in Fig. 1 gives another interpretation of the enhancement of Cooper pairing across the crossover. The effect of the attractive interaction is indicated by the ratio  $|U|/W$  for a small  $U_{\text{imp}}$ , while that should be represented by  $|U|/W_{\text{imp}}$  for a large  $U_{\text{imp}}$ , where  $W$  and  $W_{\text{imp}}$  are the width of the host band and that of the impurity band, respectively. Since  $W \gg W_{\text{imp}}$  for a small impurity concentration  $n_{\text{imp}}$ , the interaction is effectively enhanced in the impurity band region. The enhanced pairing interaction leads to the enhancement of superconductivity in the crossover regime, as shown in §5.

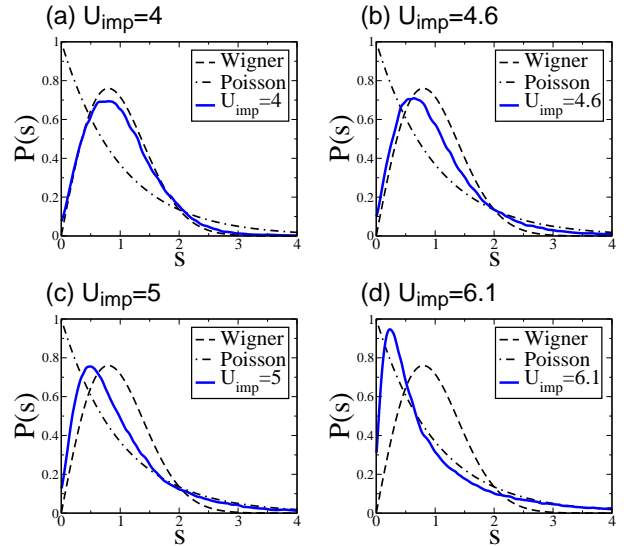


Fig. 3. Results of the level statistics for  $n_{\text{imp}} = 0.02$ . We show the nearest-level-spacing distribution function  $P(s)$  for energy levels within  $|\varepsilon_{\alpha} - \mu| < \varepsilon_c = 0.2$ . The crossover from the Wigner-Dyson statistics to the Poisson statistics occurs as the impurity potential  $U_{\text{imp}}$  increases. The numerical calculation is carried out for  $21^3$  sites and 250 samples.

Anderson localization in the crossover regime is also observed by the analysis of level statistics.<sup>44</sup> Figure 3 shows the nearest-level-spacing distribution function  $P(s)$  defined as

$$P(s) = \langle \langle \delta(|\varepsilon_{\alpha} - \varepsilon_{\alpha+1}|/\varepsilon_s - s) \rangle \rangle_{E_F}, \quad (3)$$

where  $\varepsilon_s$  is the averaged nearest level spacing. It has been shown that the distribution obeys the Poisson statistics  $P(s) = \exp(-s)$  in the insulating state, while it obeys the Wigner-Dyson statistics  $P(s) = \frac{\pi}{2}s \exp(-\pi s^2/4)$  in the

metallic state.<sup>44,45</sup> As shown in Fig. 3, the nearest-level-spacing distribution function  $P(s)$  shows a crossover from the Wigner-Dyson statistics to the Poisson statistics with increasing  $U_{\text{imp}}$  across the crossover from the host band to the impurity band. Because of the small DOS near the band edge, it is difficult to carry out finite-size scaling.<sup>44</sup> However, it is clear that the Anderson transition occurs in the crossover regime at around  $U_{\text{imp}} = 4.6$ , consistent with the analysis of IPR.

## 5. Superconductivity

### 5.1 Formulation

Next, we discuss the superconductivity. We adopt real-space self-consistent T-matrix approximation (RSTA) to analyze the model eq. (1). The RSTA has been formulated for disordered  $d$ -wave superconductivity in high- $T_c$  cuprates.<sup>46</sup> The thermal fluctuation of superconductivity is taken into account in the self-consistent 1-loop order. Because the calculation is carried out in real space, randomness is accurately taken into account.

Most microscopic studies of superconductivity in random systems have been based on mean field approximation.<sup>10,47-49</sup> However, the fluctuation plays an important role in strongly disordered systems because the fluctuation is enhanced by microscopic inhomogeneity.<sup>10,46</sup> RSTA can be carried out in more than  $10^3$  sites, which is needed for the analysis of three-dimensional models. We carry out a numerical calculation in a  $11 \times 11 \times 11$  lattice, unless otherwise mentioned. This lattice size is much larger than the limit of quantum<sup>12</sup> and classical<sup>13</sup> Monte Carlo simulations.

The formulation of RSTA is described as follows. We diagonalize the non-interacting Hamiltonian

$$H_0 = -t \sum_{\langle i,j \rangle, \sigma} c_{i\sigma}^\dagger c_{j\sigma} + \sum_i (W_i - \mu) n_i, \quad (4)$$

and obtain the undressed Green function as

$$G_0(\vec{r}, \vec{r}', \omega_n) = \sum_\alpha \psi_\alpha(\vec{r}) \frac{1}{i\omega_n - \varepsilon_\alpha} \psi_\alpha^*(\vec{r}'), \quad (5)$$

where  $\omega_n = (2n+1)\pi T$  is the Matsubara frequency.

The Dyson equation is expressed as

$$G(\vec{r}, \vec{r}', \omega_n) = G_0(\vec{r}, \vec{r}', \omega_n) + \sum_{\vec{r}_1, \vec{r}_2} G_0(\vec{r}, \vec{r}_1, \omega_n) \Sigma(\vec{r}_1, \vec{r}_2, \omega_n) G(\vec{r}_2, \vec{r}', \omega_n), \quad (6)$$

where  $\Sigma(\vec{r}_1, \vec{r}_2, \omega_n)$  is the self-energy represented in real space. We estimate self-energy using the self-consistent 1-loop-order approximation, whose results in the clean limit have been summarized in ref. 50. We adopt quasi-static approximation<sup>51-55</sup> as in ref. 46, where quantum fluctuation is ignored, but thermal fluctuation is appropriately taken into account. We have quantitatively shown the validity of quasi-static approximation as well as self-consistent 1-loop-order approximation for superconducting fluctuation.<sup>55</sup> Note that the characteristic dynamical property of superconducting fluctuation leads to the validity of quasi-static approximation.<sup>55</sup>

Self-energy is given as

$$\Sigma(\vec{r}, \vec{r}', \omega_n) = -TU^2 T(\vec{r}, \vec{r}') G(\vec{r}', \vec{r}, -\omega_n). \quad (7)$$

The propagator of superconducting fluctuation, namely, the T-matrix, is obtained using

$$T(\vec{r}, \vec{r}') = T_0(\vec{r}, \vec{r}') - \sum_{\vec{r}_1} UT_0(\vec{r}, \vec{r}_1) T(\vec{r}_1, \vec{r}'), \quad (8)$$

$$T_0(\vec{r}, \vec{r}') = T \sum_n G(\vec{r}, \vec{r}', \omega_n) G(\vec{r}, \vec{r}', -\omega_n) \phi(\omega_n)^2, \quad (9)$$

where we take into account the cutoff frequency as  $\phi(\omega) = [1 + \exp\{a(|\omega|/\omega_c - 1)\}]^{-1}$  with  $a = 20$ . We assume the cutoff frequency  $\omega_c = 0.2$  in accordance with the phonon frequency  $\omega_{\text{ph}} \sim 150$  meV in B-doped diamond.<sup>39</sup> The T-matrix diverges at the superconducting transition temperature. This criterion gives rise to the transition temperature of the BCS theory, namely, the mean field theory with respect to  $U$ , when we neglect self-energy.

Since the random potential is included in the unperturbed Hamiltonian  $H_0$ , randomness is accurately taken into account in RSTA. The spatial dependences of superconducting fluctuation and single-particle states are self-consistently determined. We find that perturbative approximations for randomness, such as the Born approximation,<sup>56</sup> CPA,<sup>31</sup> and T-matrix approximation,<sup>57-59</sup> break down for a large impurity potential  $U_{\text{imp}} > 4$ . This is because the quasiparticle states around the Fermi level mainly consist of impurity states whose wave function is localized around impurity sites. Impurity potential should be taken into account in zeroth-order approximation when the impurity band plays an essential role in superconductivity.

### 5.2 Microscopic inhomogeneity

First, we investigate the spatial inhomogeneity of superconducting susceptibility defined as

$$\chi_{\text{sc}}(\vec{r}) = \sum_{\vec{r}'} T(\vec{r}, \vec{r}'), \quad (10)$$

which is spatially uniform in the clean limit. A typical spatial dependence of  $\chi_{\text{sc}}(\vec{r})$  is shown in Fig. 4 for various  $U_{\text{imp}}$  values. Since it is difficult to show the spatial dependence in the entire three-dimensional lattice,  $\vec{r} = (x, y, z)$ , we show the spatial dependence on the plane  $z = 1$ .

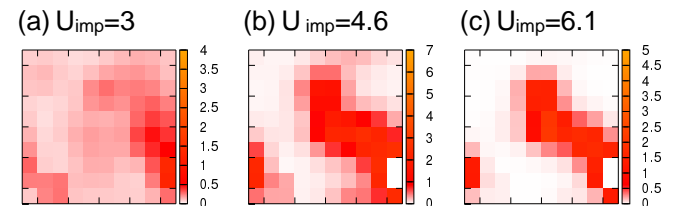


Fig. 4. Typical spatial dependences of the superconducting susceptibility  $\chi_{\text{sc}}(\vec{r})$  for (a)  $U_{\text{imp}} = 3$ , (b)  $U_{\text{imp}} = 4.6$ , and (c)  $U_{\text{imp}} = 6.1$ . We assume  $n_{\text{imp}} = 0.02$ ,  $T = 0.002$ , and  $U = -1$ . We show the results on the plane at  $z = 1$  in the three-dimensional lattice.

In Figs. 4(a)-4(c), the superconducting correlation develops in the “dirty region” that includes many impurities, in contrast to the conventional spatial dependence, in which superconductivity is suppressed by the impurities.<sup>10,46-49</sup> This is because the wave functions of quasiparticle states around the Fermi level have a large weight around impurity sites, and therefore, impurity sites play more important roles in superconductivity than host sites regardless of  $U_{\text{imp}} > 0$ . Thus, a unique spatial structure of superconductivity is realized in heavily doped semiconductors. The  $s$ -wave symmetry of superconductivity is essential for this result, as discussed in §7.

The spatial inhomogeneity of the superconducting correlation, namely, the mesoscopic fluctuation<sup>60</sup> increases with increasing  $U_{\text{imp}}$ . Superconductivity is spatially homogeneous in the host band regime  $U_{\text{imp}} < 4$ , but significantly inhomogeneous in the impurity band regime  $U_{\text{imp}} > 5$ , as shown in Fig. 4. The microscopic inhomogeneity of the superconducting correlation can be regarded as the localization of Cooper pairs.<sup>11</sup> Figure 4 indicates that the Anderson localization of single-particle states is accompanied by the localization of Cooper pairs. A similar microscopic inhomogeneity has been discussed for high- $T_c$  cuprates from both experimental<sup>61</sup> and theoretical points of view.<sup>13,46-49,62,63</sup>

### 5.3 Superconducting fluctuation and pseudogap

The spatial inhomogeneity of the order parameter generally disturbs the long-range coherence of superconductivity. Then, the short-range correlation induces a pseudogap in the excitation spectrum. In other words, the fluctuation is enhanced by the localization of Cooper pairs, and therefore the precursor of superconductivity appears above  $T_c$ .

Figure 5 shows the DOS above  $T_c$ , which is obtained using

$$\rho(\omega) = \left\langle -\frac{1}{\pi N} \sum_{\vec{r}} \text{Im} G^{\text{R}}(\vec{r}, \vec{r}, \omega) \right\rangle_{\text{av}}, \quad (11)$$

where  $\langle \rangle_{\text{av}}$  denotes the random average. We take the random average for 10 samples of the impurity distribution. We find that the DOS is self-averaged, and therefore the sample dependence is weak for the spatially averaged DOS. We see that the effect of superconducting fluctuation is negligible in the host band regime ( $U_{\text{imp}} = 4$ ), while the pseudogap is induced by a short-range superconducting fluctuation in the crossover and impurity regimes ( $U_{\text{imp}} = 4.6, 5$ , and  $6.1$ ). It is shown that the pseudogap increases with increasing impurity potential, and therefore the DOS at the Fermi energy is significantly suppressed in the impurity band regime above  $T_c$ .

We explain here the mechanism of pseudogap in detail. (1) The small width of the impurity band leads to a small Fermi energy, and therefore a small coherence length. A pseudogap generally appears in small-coherence-length superconductors, such as high- $T_c$  cuprates and organic superconductors.<sup>50</sup> (2) The fractal structure of the single-particle wave function enhances the pseudogap, as discussed by Feigel'man *et al.*<sup>11</sup> (3) The localization of Cooper pairs, namely, the microscopic inhomogeneity of

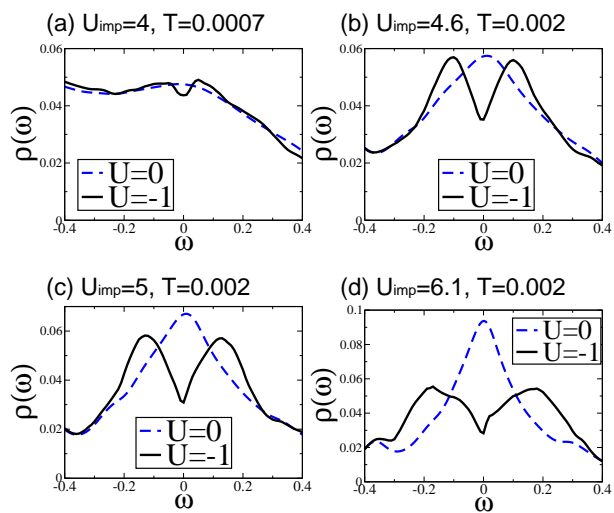


Fig. 5. DOS's for various impurity potentials  $U_{\text{imp}}$  (solid lines). We choose the temperature close to the critical point of the superconductivity,  $T = 0.0007$  for  $U_{\text{imp}} = 4$ , and  $T = 0.002$  for  $U_{\text{imp}} = 4.6, 5$ , and  $6.1$ . We take the random average over 10 samples of the impurity distribution. We assume  $n_{\text{imp}} = 0.02$  and  $U = -1$ . The bare DOS at  $U = 0$  is shown for a comparison (dashed lines).

superconductivity enhances the thermal fluctuation and also the pseudogap.<sup>46</sup> (4) The effective pairing interaction for the  $s$ -wave superconductivity is enhanced by the localization of single particle-states, as discussed in §4. The transition temperature in the mean field theory  $T_c^{\text{MF}}$  with respect to  $U$ , where the fluctuation is neglected, increases with increasing impurity potential  $U_{\text{imp}}$ . These features give rise to the pseudogap in the crossover and impurity band regimes.

The pseudogap disappears in the host band regime because of the wide host band of diamond, the extended wave function of quasiparticle states, and the spatially homogeneous superconducting correlation. Thus, the crossover from host band superconductivity to impurity band superconductivity is accompanied by the crossover from the conventional Fermi liquid state to the pseudogap state.

A large attractive interaction  $U = -9.2$  gives rise to the transition temperature  $T_c \sim 0.002$  in the clean limit ( $U_{\text{imp}} = 0$ ). We confirmed that the superconducting fluctuation is negligible for these parameters. The thermal fluctuation at  $T = 0.002$  hardly affects the DOS in the absence of disorders. This means that randomness plays an essential role in the pseudogap in the crossover and impurity band regimes.

### 5.4 Superconducting susceptibility

We investigate here the superconducting susceptibility averaged over real space as well as the randomness

$$\chi_{\text{sc}} = \left\langle \frac{1}{N} \sum_{\vec{r}} \chi_{\text{sc}}(\vec{r}) \right\rangle_{\text{av}}. \quad (12)$$

This susceptibility diverges at the critical point of superconductivity. Although the superconducting susceptibility is always finite in our calculation due to the finite size



effect, the magnitude of  $\chi_{sc}$  indicates the closeness to the critical point.

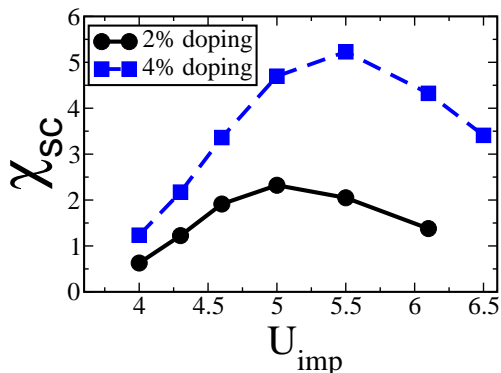


Fig. 6. Superconducting susceptibility  $\chi_{sc}$ . We show the  $U_{imp}$  dependences for  $n_{imp} = 0.02$  (circles) and  $n_{imp} = 0.04$  (squares), respectively. We assume  $T = 0.002$  and  $U = -1$ .

Figure 6 shows the  $U_{imp}$  dependences of  $\chi_{sc}$  for  $n_{imp} = 0.02$  and  $n_{imp} = 0.04$ . We see the dome shape of superconducting susceptibility against the impurity potential for a fixed impurity concentration. The peak appears in the crossover regime. These results indicate that the optimum  $T_c$  is obtained in the crossover regime.

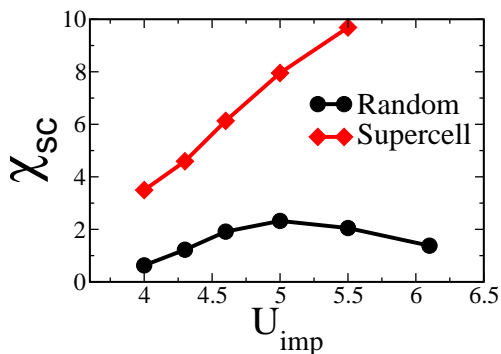


Fig. 7. Superconducting susceptibility  $\chi_{sc}$  estimated for the supercell (diamonds). We put the impurities at  $\vec{r} = (3l + 1, 3m + 1, 3n + 1)$  with  $l$ ,  $m$ , and  $n$  being integers. The impurity concentration is  $n_{imp} = 0.0203$  for the  $11 \times 11 \times 11$  lattice. The  $\chi_{sc}$  in the random system with  $n_{imp} = 0.02$  is shown for comparison (circles). We assume  $T = 0.002$  and  $U = -1$ .

The randomness is essential for the dome shape of the superconducting susceptibility in Fig. 6. To illuminate this point, we show the superconducting susceptibility  $\chi_{sc}$  in the supercell, in which impurities are set at  $\vec{r} = (3l + 1, 3m + 1, 3n + 1)$ . Figure 7 shows the comparison between the supercell and the random system. We see that the susceptibility  $\chi_{sc}$  monotonically increases in the supercell with increasing  $U_{imp}$ , in contrast to the random system. Thus, the suppression of the superconductivity in the impurity band regime rather arises from randomness.

The enhancement of superconductivity in the supercell has been pointed out by Shirakawa *et al.*<sup>31</sup> on the basis

of the CPA. Our results are consistent with their claim. However, superconductivity is enhanced in the supercell in our calculation because fluctuation, which is not taken into account in the CPA, is suppressed.

We have confirmed that the transition temperature in the mean field theory,  $T_c^{MF}$ , monotonically increases with increasing impurity potential  $U_{imp}$  owing to the enhancement of pairing interaction, as discussed in §4. On the other hand, superconducting susceptibility is suppressed by mesoscopic and thermal fluctuations in the crossover and impurity band regimes. Thus, the competition between the enhancement of Cooper pairing and that of superconducting fluctuations gives rise to the dome shape of superconducting susceptibility in Fig. 6.

The long-range coherence of superconductivity is hardly realized in the impurity band regime because of the localization of Cooper pairs (see §5.2). The susceptibility defined in eqs. (10) and (12) takes into account both the short-range and long-range correlation of superconductivity. The weight of the short-range and long-range correlation can be clarified by analyzing the averaged correlation function

$$T_{av}(\vec{r}) = \left\langle \frac{1}{N} \sum_{\vec{r}'} T(\vec{r}' + \vec{r}, \vec{r}') \right\rangle_{av}. \quad (13)$$

We have confirmed that the correlation function increases for a small  $|\vec{r}|$  in the impurity band regime, but then decreases for a large  $|\vec{r}|$  with increasing  $U_{imp}$ . This means that the short-range correlation develops, but the long-range correlation is suppressed in the impurity band regime, as we have mentioned above.

Figure 6 shows that the peak of  $\chi_{sc}$  shifts to the impurity band regime with increasing impurity concentration  $n_{imp}$ . This is because Anderson localization is suppressed by increasing the concentration of carriers,  $n_{imp}$ , and then superconducting fluctuation is also suppressed. The pseudogap is suppressed by increasing  $n_{imp}$ , while the  $T_c$  is increased, as will be shown in Figs. 9-11.

### 5.5 Phase diagram

We illustrate here a schematic figure of the phase diagram against the impurity potential  $U_{imp}$  and the temperature  $T$  (Fig. 8).

As we have discussed in §4, the pairing interaction is effectively enhanced by the localization of single-particle wave functions with increasing  $U_{imp}$ . Therefore, the transition temperature  $T_c^{MF}$  in the mean field theory and the magnitude of superconducting gap  $\Delta$  at  $T = 0$  monotonically increase with increasing impurity potential  $U_{imp}$  (dashed line in Fig. 8). We have confirmed this  $U_{imp}$  dependence of the superconducting gap in the mean field theory at  $T = 0$ .

The Anderson localization of single-particle wave functions leads to microscopic inhomogeneity, which enhances the thermal fluctuation in superconductivity. Then, the long-range coherence is disturbed, as shown in §5.4. The competition between the enhancement of the effective pairing interaction and that of superconducting fluctuations leads to a dome shape of the superconducting state with a peak  $T_c$  in the crossover regime (solid

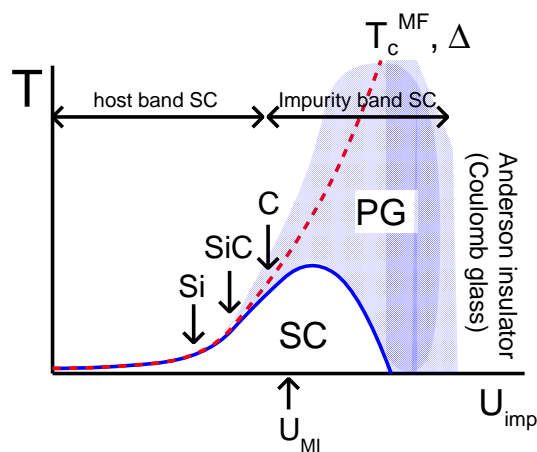


Fig. 8. Schematic figure of the phase diagram against the impurity potential  $U_{\text{imp}}$  and the temperature  $T$ . The crossover from the host band to the impurity band is described. The solid line shows the transition temperature  $T_c$  of superconductivity. The dashed line shows the transition temperature  $T_c^{\text{MF}}$  in the mean field theory. The shaded region indicates the pseudogap state induced by the incoherent Cooper pairs. The upward arrow ( $U_{\text{MI}}$ ) shows the virtual quantum metal-insulator transition in the absence of superconductivity. The downward arrows indicate our interpretation for B-doped diamond, SiC, and Si (see §6).

line in Fig. 8).

The short-range correlation of superconductivity gives rise to the resonance scattering between incoherent Cooper pairs and quasiparticles, which leads to a pseudogap in the shaded region in Fig. 8. In other words, the superconducting gap obtained in the mean field theory is changed to a pseudogap by the fluctuations.

The pseudogap state would be an insulating state in the highly disordered regime because both electrons and Cooper pairs are localized. This state is regarded as the “hard gap insulator” proposed by Feigel’man *et al.*,<sup>11</sup> which seems to be realized in the disordered thin films.<sup>64–75</sup> Thus, the insulating state near the SIT is expected to be the localized Cooper pairing state, but not the Coulomb glass state.<sup>76</sup>

### 5.6 Doping dependence

We investigate here the doping dependence. Impurity level depends on the impurity concentration  $n_{\text{imp}}$  in the heavily doped semiconductors, but we show the results for a fixed  $U_{\text{imp}}$  for simplicity.

Figure 9 shows the doping dependence of the Fourier-transformed correlation function

$$T_{\text{av}}^q(\vec{q}) = \int T_{\text{av}}(\vec{r}) e^{i\vec{q}\vec{r}} d\vec{r}. \quad (14)$$

The spatially averaged superconducting susceptibility  $\chi_{\text{sc}}$  is related to this correlation function as  $\chi_{\text{sc}} = T_{\text{av}}^q(0)$ . We see that the correlation function increases at  $\vec{q} = 0$  with increasing doping concentration; it hardly changes at  $\vec{q} \neq 0$ . This means that the long-range correlation of superconductivity develops in the heavily doped regime. This is consistent with the experimental observation that the  $T_c$  of B-doped diamond increases with increasing concentration of isolated boron acceptors.<sup>21, 22, 41</sup>

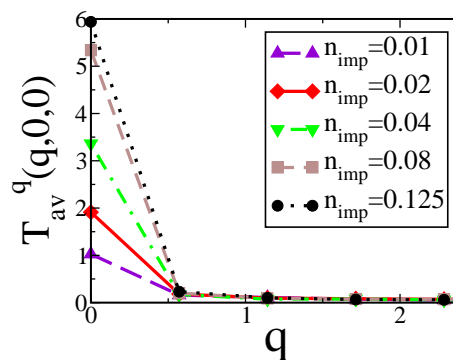


Fig. 9. Fourier-transformed correlation function  $T_{\text{av}}^q(\vec{q})$  along  $\vec{q} = q\hat{x}$  for  $n_{\text{imp}} = 0.01, 0.02, 0.04, 0.08,$  and  $0.125$  from the bottom to the top. We assume  $U_{\text{imp}} = 4.6$ ,  $U = -1$ , and  $T = 0.002$ .

It has been pointed out that the concentration of carriers is different from that of boron atoms owing to the presence of the B-H complex and/or the B-B dimer.<sup>41, 77</sup> We have confirmed that the B-H complex as well as the B-B dimer neither enhance nor suppress superconductivity. Therefore, the doping concentration  $n_{\text{imp}}$  discussed in this paper should be regarded as the concentration of isolated boron acceptors, consistent with the experimental observation.<sup>41</sup>

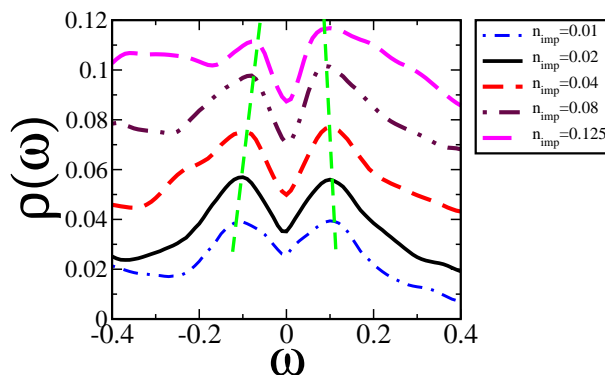


Fig. 10. DOS's for  $n_{\text{imp}} = 0.01, 0.02, 0.04, 0.08,$  and  $0.125$  from the bottom to the top. We assume that  $U_{\text{imp}} = 4.6$ ,  $U = -1$ , and  $T = 0.002$ . The vertical dashed line is drawn to emphasize the doping dependence of the gap in DOS.

Figure 10 shows the doping dependence of the DOS in the crossover regime ( $U_{\text{imp}} = 4.6$ ). We see that the pseudogap is suppressed by increasing the doping concentration  $n_{\text{imp}}$ , although the superconducting correlation is enhanced, as shown in Fig. 9. The single-particle states around the Fermi level become itinerant with increasing  $n_{\text{imp}}$  owing to the percolation of impurity states. Then, Anderson localization is suppressed, and therefore superconducting fluctuation is suppressed.

The schematic figure of the doping dependence in the crossover regime is shown in Fig. 11(a). We would like to stress again that the transition temperature  $T_c$  of superconductivity increases, but the thermal fluctuation is suppressed by acceptor doping. The pseudogap and superconducting gap decrease in contrast to  $T_c$  with

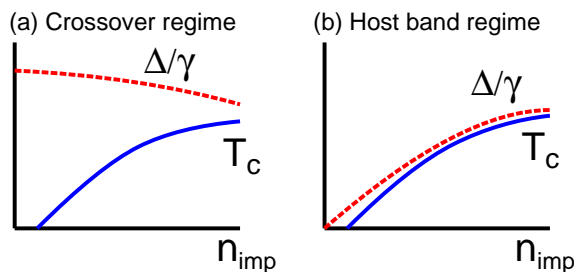


Fig. 11. Schematic figure of the doping dependence in (a) the crossover regime and (b) the host band regime, respectively. We show the magnitude of the superconducting gap (or pseudogap) divided by  $\gamma = 1.73$  for a comparison with  $T_c$ .

increasing doping concentration. These features in the crossover regime should be contrasted to those in the host band regime where the thermal fluctuation is negligible except at a very low concentration of carriers. A conventional doping dependence is expected in the host band regime; superconducting gap increases together with  $T_c$ , as shown in Fig. 11(b).

We have investigated the effect of doping compensation due to doped donors and carrier increase due to the additional acceptors. We found that superconductivity is significantly suppressed.<sup>78</sup> In other words, high  $T_c$  of superconductivity is expected in uncompensated semiconductors with large carrier concentration.

## 6. Interpretation for B-doped Diamond, SiC and Si

We discuss here B-doped diamond, SiC, and Si on the basis of the results in §5. Since no clear impurity band is observed in the angle-resolved photoemission spectroscopy (ARPES),<sup>27</sup> B-doped diamond does not seem to be in the impurity band regime. On the other hand, the high transition temperature  $T_c > 10$  K,<sup>21,22</sup> high upper critical field  $H_{c2} > 10$  T,<sup>21,22,26</sup> and large Ginzburg-Landau (GL) parameter  $\kappa \sim 18$ <sup>26</sup> imply that B-doped diamond is close to or in the crossover regime. In general, the localization of single-particle wave functions leads to a small coherence length and a low superfluid density. Therefore, a high upper critical field  $H_{c2}$  and a large GL parameter  $\kappa$  are expected in the crossover regime. The localization effect revealed by electric resistivity measurements<sup>21,25</sup> also indicates that B-doped diamond is close to the crossover regime.

These observations should be contrasted to those of B-doped SiC. B-doped SiC is a type I superconductor whose critical field  $H_c$  is  $10^{-3}$  times less than the upper critical field of B-doped diamond.<sup>19</sup> Its GL parameter  $\kappa \sim 0.35$ <sup>19,40</sup> is much less than that of B-doped diamond. A small residual resistivity implies that the effect of Anderson localization is negligible for superconductivity in B-doped SiC. These marked differences between diamond and SiC indicate that B-doped SiC is in the host band regime far from the crossover regime. This is consistent with the acceptor level of boron atoms in the SiC  $\sim 0.3$  eV,<sup>20,79</sup> which is smaller than that in diamond. It is expected that the B-doped Si is far from the crossover regime because its acceptor level of  $\sim 0.045$  eV<sup>20,80</sup> is

the smallest among those of diamond, SiC, and Si. We have illustrated these interpretations in Fig. 8.

Before closing the section, we will comment on the difference between B-doped SiC and Al-doped SiC. Both compounds have similar  $T_c$  values of  $\sim 1.5$  K. However, Al-doped SiC seems to be a type II superconductor with  $\kappa \sim 1.8$  in contrast to B-doped SiC being a type I superconductor. Since the acceptor level of Al-doped SiC of  $\sim 0.2$  eV is smaller than that of B-doped SiC, the difference in the GL parameter  $\kappa$  seems to be incompatible with the interpretation based on Fig. 8. However, the difference between B-doped SiC and Al-doped SiC may be understood in the following way. We expect that silicon sites play more important roles in the superconductivity than carbon sites, because the DOS at the Fermi level mainly arises from silicon sites.<sup>20</sup> It has been pointed out that boron atoms mainly substitute for carbon atoms.<sup>20</sup> If aluminium atoms substitute for silicon atoms rather than for carbon atoms, the random potential due to substitutional aluminum acceptors will affect superconductivity more significantly than that due to boron acceptors. Then, type II superconductivity can occur in Al-doped SiC. Further studies are desired to examine this possibility.

## 7. Similarity to High- $T_c$ Cuprates

We point out the close relationship between doped semiconductors and high- $T_c$  cuprates. We see the similarity between Fig. 8 and the typical phase diagram of high- $T_c$  cuprates. *s*-Wave superconductivity and Anderson localization in doped semiconductors correspond to *d*-wave superconductivity and the antiferromagnetic Mott insulator in high- $T_c$  cuprates, respectively. The host band and impurity band regimes in the former correspond to the overdoped and underdoped regimes in the latter, respectively.

We have claimed that the pseudogap in the underdoped high- $T_c$  cuprates is a precursor of superconductivity.<sup>50,81,82</sup> The pseudogap due to the same mechanism has been discussed for the doped semiconductors in this paper. The same mechanism of the pseudogap has also been proposed to high-density quark matters.<sup>83</sup> Note that the pseudogap in these systems does not arise from the shift in chemical potential, which describes the BCS-BEC crossover in zeroth-order approximation.<sup>84-86</sup> In general, the shift in chemical potential is quantitatively important in low-density systems, such as trapped cold fermion gases,<sup>87</sup> while higher-order corrections, namely, resonance scattering between incoherent Cooper pairs and quasiparticles, play an essential role in high-density systems.<sup>50</sup> Although a doped semiconductor seems to be a low-density system, its density is effectively high in the impurity band regime because the impurity band is nearly half-filled. Actually, the shift in chemical potential is negligible in our calculation. The BCS-BEC crossover described by the shift in chemical potential was first proposed for superconductivity in semiconductors.<sup>84</sup> However, this is not the case in our calculation.

Many lines of experimental evidence have been obtained for microscopic inhomogeneity in high- $T_c$  cuprates.<sup>61</sup> According to the results of RSTA, the mi-



microscopic inhomogeneity generally appears in small-coherence-length non- $s$ -wave superconductors.<sup>46</sup> In contrast to that of the  $s$ -wave superconductor discussed in this paper, the microscopic inhomogeneity of non- $s$ -wave superconductors is not necessarily accompanied by the localization of quasiparticles. A weak disorder leads to microscopic inhomogeneity in the non- $s$ -wave superconductor with a small coherence length. On the other hand, the  $s$ -wave superconductivity is robust against nonmagnetic disorders in accordance with the Anderson theorem<sup>88</sup> until Anderson localization occurs.

We note that the microscopic inhomogeneity of high- $T_c$  cuprates is enhanced by the multi-criticality of antiferromagnetism and  $d$ -wave superconductivity.<sup>63</sup> An antiferromagnetic correlation develops in the “dirty region”, while a local superconductivity occurs in the “clean region”. It is expected that the insulating state near the SIT in high- $T_c$  cuprates is neither the simple Mott insulator nor the Anderson insulator in analogy with the doped semiconductors discussed in §5.5. It is expected that the localized Cooper pairing state is realized in a variety of systems near the SIT.

## 8. Summary and Discussion

We have investigated localization and superconductivity in doped semiconductors on the basis of the disordered attractive Hubbard model in three dimensions. We focused on the crossover from the superconductivity in the host band to that in the impurity band. Anderson localization is accompanied by the crossover. We found that the effective interaction for the pairing is enhanced in the crossover regime. The superconducting correlation is enhanced in the crossover regime, but suppressed by the mesoscopic and thermal fluctuations in superconductivity with approach to the impurity band regime. The dome shape of the superconducting state is expected in the phase diagram against the impurity potential  $U_{\text{imp}}$  and the temperature  $T$ . The long-range coherence is destroyed in the impurity band regime, and then the short-range correlation leads to a pseudogap. The insulating state due to the localization of Cooper pairs is expected to be realized in the highly disordered regime.

We proposed that the marked differences between B-doped diamond, SiC, and Si are understood by taking into account the impurity potential of these compounds, which are determined by the acceptor level in the lightly doped region. B-doped diamond is close to or in the crossover regime, while the others are in the host band regime far away from the crossover regime. The experimental results on transition temperature, critical magnetic field, residual resistivity, and the feature of the SIT are consistent with our interpretation.

Two mechanisms have been proposed for the SIT in  $s$ -wave superconductors. One is the so-called fermionic effect, which arises from the long-range Coulomb interaction.<sup>5–7,9</sup> The other is the bosonic effect, namely, the fluctuations in superconductivity.<sup>8,10,11,13–16</sup> Although the SIT in some bulk materials can be understood by taking the fermionic effect into account,<sup>24</sup> the bosonic effect has been indicated by the recent experiments on disordered thin films, such as Bi, InO<sub>x</sub>, and TiN films.<sup>16,66–75</sup>

We have pointed out that a significant bosonic effect appears in a doped wide-gap semiconductor, which may be realized in B-doped diamond.

In summary, we have investigated superconductivity and localization with focus on the crossover from the host band regime to the impurity band regime in doped semiconductors. The superconducting correlation is enhanced in the crossover regime where the electrons have a dual nature, namely, the itinerant and localized characters. Anderson localization in the crossover regime is accompanied by the mesoscopic and thermal superconducting fluctuations in superconductivity. The similarity of doped semiconductors to high- $T_c$  cuprates and disordered thin films has been discussed.

## Acknowledgments

The authors are grateful to J. Akimitsu, N. Hayashi, K. Ishizaka, M. Kriener, Y. Maeno, H. Mukuda, T. Muranaka, J. Nakamura, N. Nishida, T. Nishizaki, Y. Ohta, T. Shirakawa, Y. Takano, T. Wakita, and T. Yokoya for valuable discussions. This study was financially supported by the Nishina Memorial Foundation and Grants-in-Aid for Young Scientists (B) and for Scientific Research on Priority Areas (No. 17071002) from MEXT, Japan. Numerical computation in this work was partly carried out at the Yukawa Institute Computer Facility.

- 1) J. G. Bednorz and K. A. Müller: *Z. Phys. B* **64** (1986) 189.
- 2) K. Kanoda: *J. Phys. Soc. Jpn.* **75** (2006) 051007 and references therein.
- 3) For a review, Y. Kitaoka, S. Kawasaki, T. Mito, and Y. Kawasaki: *J. Phys. Soc. Jpn.* **74** (2005) 186; J. Flouquet, G. Knebel, D. Braithwaite, D. Aoki, J. P. Brison, F. Hardy, A. Huxley, S. Raymond, B. Salce, and I. Sheikin: *cond-mat/0505713*.
- 4) E. Abrahams, P. W. Anderson, D. C. Licciardello, and T. V. Ramakrishnan: *Phys. Rev. Lett.* **42** (1979) 673.
- 5) S. Maekawa and H. Fukuyama: *J. Phys. Soc. Jpn.* **51** (1982) 1380.
- 6) H. Takagi and Y. Kuroda: *Prog. Theore. Phys.* **69** (1983) 1677; *Solid State Com.* **41** (1982) 643.
- 7) A. M. Finkel'stein: *Pis'ma Zh. Eksp. Teor. Fiz.* **45** (1987) 37 [*JETP Lett.* **45** (1987) 46.]
- 8) M. P. A. Fisher, P. B. Weichman, G. Grinstein, and D. S. Fisher: *Phys. Rev. B* **40** (1989) 546; M. P. A. Fisher: *Phys. Rev. Lett.* **65** (1990) 923; M.-C. Cha, M. P. A. Fisher, S. M. Girvin, M. Wallin, and A. P. Young: *Phys. Rev. B* **44** (1991) 6883.
- 9) H. Ishida and R. Ikeda: *J. Phys. Soc. Jpn.* **67** (1998) 983.
- 10) A. Ghosal, M. Randeria, and N. Trivedi: *Phys. Rev. Lett.* **81** (1998) 3940; *Phys. Rev. B* **63** (2000) 020505; *Phys. Rev. B* **65** (2001) 014501.
- 11) M. V. Feigel'man, L. B. Ioffe, V. E. Kravtsov, and E. A. Yuzbashyan: *Phys. Rev. Lett.* **98** (2007) 027001; see also M. V. Feigel'man, L. B. Ioffe, and E. A. Yuzbashyan: *cond-mat/0504766*.
- 12) D. Hurt, E. Odabashian, W. E. Pickett, R. T. Scalettar, F. Mondaini, T. Paiva, and R. R. dos Santos: *Phys. Rev. B* **72** (2005) 144513 and references therein.
- 13) Y. Dubi, Y. Meir, and Y. Avishai: *Nature* **449** (2007) 876.
- 14) B. I. Shklovskii: *Phys. Rev. B* **76** (2007) 224511.
- 15) I. S. Beloborodov, A. L. Lopatin, V. M. Vinokur, and K. B. Efetov: *Rev. Mod. Phys.* **79** (2007) 469.
- 16) V. Vinokur, T. I. Baturina, M. V. Fitsul, A. Yu. Mironov, M. R. Baklanov, and C. Strunk: *Nature* **452** (2008) 613; M. V. Fitsul, V. Vinokur, and T. I. Baturina: *Phys. Rev. Lett.* **100** (2008) 086805; See also K. B. Efetov, M. V. Feigel'man, and P. B. Wiegmann: *arXiv:0804.3775*.

- 17) E. A. Ekimov, V. A. Sidorov, E. D. Bauer, N. N. Mel'nik, N. J. Curro, J. D. Thompson, and S. M. Stishov: *Nature* (London) **428** (2004) 542.
- 18) E. Bustarret, C. Marcenat, P. Achatz, J. Kacmarcik, F. Levy, A. Huxley, L. Ortéga, E. Bourgeois, X. Blase, D. Débarre, and J. Boulmer: *Nature* **444** (2006) 465.
- 19) Z.-A. Ren, J. Kato, T. Muranaka, J. Akimitsu, M. Kriener, and Y. Maeno: *J. Phys. Soc. Jpn.* **76** (2007) 103710.
- 20) T. Muranaka: private communication.
- 21) Y. Takano, T. Takenouchi, S. Ishii, S. Ueda, T. Okutsu, I. Sakaguchi, H. Umezawa, H. Kawarada, M. Tachiki: *Diam. Relat. Mater.* **16** (2007) 911.
- 22) Y. Takano: *Sci. Technol. Adv. Mater.* **7** (2006) S1.
- 23) T. F. Rosenbaum, K. Andres, G. A. Thomas, and R. N. Bhatt, *Phys. Rev. Lett.* **45** (1980) 1723; S. Katsumoto, F. Komori, N. Sano, and S. Kobayashi: *J. Phys. Soc. Jpn.* **56** (1987) 2259; M. Watanabe, Y. Ootuka, K. M. Itoh, and E. E. Haller: *Phys. Rev. B* **58** (1998) 9851 and references therein.
- 24) For a review, D. Belitz, and T. R. Kirkpatrick: *Rev. Mod. Phys.* **66** (1994) 261; P. A. Lee and T. V. Ramakrishnan: *Rev. Mod. Phys.* **57** (1985) 287.
- 25) K. Ishizaka, R. Eguchi, S. Tsuda, T. Yokoya, T. Kiss, T. Shimojima, T. Togashi, S. Watanabe, C.-T. Chen, C. Q. Zhang, Y. Takano, M. Nagao, I. Sakaguchi, T. Takenouchi, H. Kawarada, and S. Shin: *Phys. Rev. Lett.* **98** (2007) 047003.
- 26) V. A. Sidorov, E. A. Ekimov, S. M. Stishov, E. D. Bauer, and J. D. Thompson: *Phys. Rev. B* **71** (2005) 060502 and *Phys. Rev. B* **74** (2006) 229903(E).
- 27) T. Yokoya, T. Nakamura, T. Matsushita, T. Muro, Y. Takano, M. Nagao, T. Takenouchi, H. Kawarada, and T. Oguchi: *Nature* **438** (2005) 648.
- 28) H. Fukuyama: *J. Supercond. Nov. Magn.* **19** (2006) 201.
- 29) G. Baskaran: *J. Supercond. Nov. Magn.* **21** (2008) 45; *Sci. Technol. Adv. Mater.* **7** (2006) S49.
- 30) M. Alaei, S. A. Jafari, and H. Akbarzadeh: *J. Phys. Chem. Solids* (2008), doi:10.1016/j.jpcs.2008.06.103.
- 31) T. Shirakawa, S. Horiuchi, Y. Ohta, and H. Fukuyama: *J. Phys. Soc. Jpn.* **76** (2007) 014711.
- 32) L. Boeri, J. Kortus, and O. K. Anderson: *Phys. Rev. Lett.* **93** (2004) 237002.
- 33) K. W. Lee and W. E. Pickett: *Phys. Rev. Lett.* **93** (2004) 237003; *Phys. Rev. B* **73** (2006) 075105.
- 34) X. Blase, C. Adessi, and D. Connétable: *Phys. Rev. Lett.* **93** (2004) 237004.
- 35) H. J. Xiang, Z. Li, J. Yang, J. G. Hou, and Q. Zhu: *Phys. Rev. B* **70** (2004) 212504.
- 36) The superconductivity in the impurity band has been proposed in 80's for Si:Au. N. Nishida, M. Yamaguchi, T. Furubayashi, K. Morigaki, H. Ishimoto, and K. Ono: *Solid State Com.* **44** (1982) 305; T. Furubayashi, N. Nishida, M. Yamaguchi, K. Morigaki, and H. Ishimoto: *Solid State Com.* **58** (1986) 587.
- 37) J. Nakamura, E. Kabasawa, N. Yamada, Y. Einaga, D. Saito, H. Isshiki, S. Yugo, and R. C. C. Perera: *Phys. Rev. B* **70** (2004) 245111.
- 38) D. Wu, Y. C. Ma, Z. L. Wang, Q. Luo, C. Z. Gu, N. L. Wang, C. Y. Li, X. Y. Lu, and Z. S. Jin: *Phys. Rev. B* **73** (2006) 012501.
- 39) M. Hoesch, T. Fukuda, J. Mizuki, T. Takenouchi, H. Kawarada, J. P. Sutter, S. Tsutsui, A. Q. R. Baron, M. Nagao, and Y. Takano: *Phys. Rev. B* **75** (2007) 140508.
- 40) M. Kriener, Y. Maeno, T. Oguchi, Z.-A. Ren, J. Kato, T. Muranaka, and J. Akimitsu: *Phys. Rev. B* **78** (2008) 024517.
- 41) H. Mukuda, T. Tsuchida, A. Harada, Y. Kitaoka, T. Takenouchi, Y. Takano, M. Nagao, I. Sakaguchi, T. Oguchi, and H. Kawarada: *Phys. Rev. B* **75** (2007) 033301.
- 42) A. K. Ramdas and S. Rodriguez: *Rep. Prog. Phys.* **44** (1981) 1297.
- 43) D. A. Parshin and H. R. Schober: *Phys. Rev. Lett.* **83** (1999) 4590; A. Mildenberger, F. Evers, and A. D. Mirlin: *Phys. Rev. B* **66** (2002) 033109 and references therein.
- 44) B. I. Shklovskii, B. Shapiro, B. R. Sears, P. Lambrianides, and H. B. Shore: *Phys. Rev. B* **47** (1993) 11487 and references therein.
- 45) B. L. Altshuler and B. I. Shklovskii: *Zh. Eksp. Teor. Fiz.* **91** (1986) 220 [*Sov. Phys. JETP* **64** (1986) 127]; B. L. Altshuler, I. Kh. Zharekeshev, S. A. Kotochigova, and B. I. Shklovskii: *Zh. Eksp. Teor. Fiz.* **94** (1988) 343 [*Sov. Phys. JETP* **67** (1988) 625]; U. Sivan and Y. Imry: *Phys. Rev. B* **35** (1987) 6074; S. N. Evangelou and E. N. Economou: *Phys. Rev. Lett.* **68** (1992) 361; E. Hofstetter and M. Schreiber: *Phys. Rev. B* **48** (1993) 16979; I. Kh. Zharekeshev and B. Kramer: *Phys. Rev. B* **51** (1995) 17239.
- 46) Y. Yanase: *J. Phys. Soc. Jpn.* **75** (2006) 124715.
- 47) M. Franz, C. Kallin, A. J. Berlinsky, and M. I. Salkola: *Phys. Rev. B* **56** (1997) 7882.
- 48) W. A. Atkinson, P. J. Hirschfeld, and A. H. MacDonald: *Phys. Rev. Lett.* **85** (2000) 3922; W. A. Atkinson, P. J. Hirschfeld, A. H. MacDonald, and K. Ziegler: *Phys. Rev. Lett.* **85** (2000) 3926.
- 49) T. S. Nunner, B. M. Andersen, A. Melikyan, and P. J. Hirschfeld: *Phys. Rev. Lett.* **95** (2005) 177003.
- 50) Y. Yanase, T. Jujo, T. Nomura, H. Ikeda, T. Hotta, and K. Yamada: *Phys. Rep.* **387** (2004) 1.
- 51) P. A. Lee, T. M. Rice, and P. W. Anderson: *Phys. Rev. Lett.* **31** (1973) 462.
- 52) M. V. Sadovskii: *Sov. Phys. JETP* **39** (1974) 845 [*Zh. Eksp. Teor. Fiz.* **66** (1974) 1720]; *Sov. Phys. Solid State* **16** (1975) 1362 [*Fiz. Tverd. Tela* **16** (1974) 2504]; *Sov. Phys. JETP* **50** (1979) 989 [*Zh. Eksp. Teor. Fiz.* **77** (1979) 2070].
- 53) O. Tchernyshyov: *Phys. Rev. B* **56** (1997) 3372.
- 54) J. Schmalian, D. Pines, and B. Stojković: *Phys. Rev. Lett.* **80** (1998) 3839; *Phys. Rev. B* **60** (1999) 667.
- 55) Y. Yanase: *J. Phys. Soc. Jpn.* **73** (2004) 1000.
- 56) A. A. Abrikosov and L. P. Gor'kov: *Sov. Phys. JETP* **12** (1961) 1243.
- 57) T. Hotta: *J. Phys. Soc. Jpn.* **62** (1993) 274.
- 58) P. J. Hirschfeld and N. Goldenfeld: *Phys. Rev. B* **48** (1993) 4219.
- 59) Y. Sun and K. Maki: *Phys. Rev. B* **51** (1995) 6059.
- 60) L. N. Bulaevskii and M. V. Sadovskii: *Pis'ma Zh. Eksp. Teor. Fiz.* **43** (1986) 76 [*JETP Lett.* **43** (1986) 99]; B. Spivak and F. Zhou: *Phys. Rev. Lett.* **74** (1995) 2800; M. A. Skvortsov and M. V. Feigel'man: *Phys. Rev. Lett.* **95** (2005) 057002.
- 61) S. H. Pan, J. P. O'Neal, R. L. Badzey, C. Chamon, H. Ding, J. R. Engelbrecht, Z. Wang, H. Eisaki, S. Uchida, A. K. Gupta, K.-W. Ng, E. W. Hudson, K. M. Lang, and J. C. Davis: *Nature* **413** (2001) 282; K. M. Lang, V. Madhavan, J. E. Hoffman, E. W. Hudson, H. Eisaki, S. Uchida and J. C. Davis: *Nature* **415** (2002) 412; K. McElroy, Jinho Lee, J. A. Slezak, D.-H. Lee, H. Eisaki, S. Uchida, and J. C. Davis: *Science* **309** (2005) 1048.
- 62) M. Mayr, G. Alvarez, A. Moreo, and E. Dagotto: *Phys. Rev. B* **73** (2006) 014509.
- 63) Y. Yanase and M. Ogata: *J. Mag. and Mag. Mat.* **310** (2007) 480.
- 64) D. B. Haviland, Y. Liu, and A. M. Goldman: *Phys. Rev. Lett.* **62** (1989) 2180.
- 65) A. F. Hebard and M. A. Paalanen: *Phys. Rev. Lett.* **65** (1990) 927.
- 66) V. F. Gantmakher, M. V. Golubkov, V. T. Dolgoplov, G. E. Tsydynzhapov, and A. A. Shashkin: *Pis'ma Zh. Eksp. Teor. Fiz.* **68** (1998) 337 [*JETP Lett.* **68** (1998) 363]; V. F. Gantmakher, M. V. Golubkov, V. T. Dolgoplov, A. A. Shashkin, and G. E. Tsydynzhapov: *Pis'ma Zh. Eksp. Teor. Fiz.* **71** (2000) 693 [*JETP Lett.* **71** (2000) 473].
- 67) G. Sambandamurthy, L. W. Engel, A. Johansson, and D. Shahar: *Phys. Rev. Lett.* **92** (2004) 107005.
- 68) M. Steiner and A. Kapitulnik: *Physica C* **422** (2005) 16.
- 69) R. Crane, N. P. Armitage, A. Johansson, G. Sambandamurthy, D. Shahar, and G. Gruner: *Phys. Rev. B* **75** (2007) 184530.
- 70) P. Spathis, H. Aubin, A. Pourret, and K. Behnia: arXiv:0712.2655.
- 71) K. H. Sarwa B. Tan, K. A. Parendo, and A. M. Goldman: *Phys. Rev. B* **78** (2008) 014506.
- 72) T. I. Baturina, C. Strunk, M. R. Baklanov, and A. Satta: *Phys. Rev. Lett.* **98** (2007) 127003; T. I. Baturina, A. Yu. Mironov, V. M. Vinokur, M. R. Baklanov, and C. Strunk: *Phys. Rev. Lett.* **99** (2007) 257003 and references therein.
- 73) B. Sacépé, C. Chapelier, T. I. Baturina, V. M. Vinokur, M. R. Baklanov, and M. Sanquer: *Phys. Rev. Lett.* **101** (2008) 157006.
- 74) K. A. Parendo, K. H. Sarwa B. Tan, and A. M. Goldman: *Phys.*

- Rev. B **76** (2007) 100508(R).
- 75) M. D. Stewart Jr., A. Yin, J. M. Xu, and J. M. Valles Jr.: Phys. Rev. B **77** (2008) 140501(R).
- 76) A. L. Efros and B. L. Shklovskii: J. Phys. **C8** (1975) L49.
- 77) J. Nakamura, N. Yamada, K. Kuroki, T. Oguchi, K. Okada, Y. Takano, M. Nagao, I. Sakaguchi, T. Takenouchi, H. Kawarada, R. C. C. Perera, and D. L. Ederer: J. Phys. Soc. Jpn. **77** (2008) 054711.
- 78) Y. Yanase and N. Yorozu: To be published in Sci. Technol. Adv. Mater.
- 79) S. Greulich-Weber: Phys. Stat. Sol. (a) **162** (1997) 95 and references therein.
- 80) G. A. Samara and C. E. Barnes: Phys. Rev. B **35** (1987) 7575 and references therein.
- 81) B. Jankó, J. Maly, and K. Levin: Phys. Rev. B **56** (1997) 11407.
- 82) Y. Yanase and K. Yamada: J. Phys. Soc. Jpn. **68** (1999) 2999.
- 83) M. Kitazawa, T. Koide, T. Kunihiro, and Y. Nemoto: Prog. Theor. Phys. **114** (2005) 117.
- 84) D. M. Eagles: Phys. Rev. **186** (1969) 456.
- 85) A. J. Leggett: *Modern Trends in the Theory of Condensed Matter*, ed. A. Pekalski and R. Przystawa (Springer-Verlag, Berlin, 1980).
- 86) P. Nozières and S. Schmitt-Rink: J. Low Temp. Phys. **59** (1985) 195.
- 87) For a review, Q. J. Chen, J. Stajic, S. N. Tan, and K. Levin: Phys. Rep. **412** (2005) 1; S. Giorgini, L. P. Pitaevskii, and S. Stringari: To be published in Rev. Mod. Phys. (arXiv:0706.3360).
- 88) P. W. Anderson: J. Phys. Chem. Solids: **11** (1959) 26.